JOURNAL OF BACTERIOLOGY, Oct. 1996, p. 5615–5626
0021-9193/96/$04.00+0

Vol. 178, No. 19

Molecular and Evolutionary Analyses of a Variable Series of Genes in *Borrelia burgdorferi* That Are Related to *ospE* and *ospF*, Constitute a Gene Family, and Share a Common Upstream Homology Box

RICHARD T. MARCONI,[1]* SHIAN YING SUNG,[1] CARRIE A. NORTON HUGHES,[2] AND JASON A. CARLYON[1]

Department of Microbiology and Immunology, Medical College of Virginia, Virginia Commonwealth University, Richmond, Virginia 23298-0678,[1] and Department of Microbiology and Immunology, School of Medicine, Georgetown University, Washington, D.C. 20007

Received 3 June 1996/Accepted 30 July 1996

In this study we report on the molecular characterization of a series of genes that constitute a gene family related to *ospE* and *ospF*. Some members of this family appear to represent recombined or variant forms of *ospE* and *ospF*. Variant *ospE* and *ospF* genes were found in several *Borrelia burgdorferi* isolates, demonstrating that their occurrence is not a phenomenon relevant to only a single isolate. Hybridization analyses revealed that the upstream sequence originally identified 5′ of the full-length *ospEF* operon exists in multiple copies ranging in number from two to six depending on the isolate. This repeated sequence, which we refer to as the upstream homology box (UHB), carries a putative promoter element. In some isolates, UHB elements were found to flank copies of *ospE* and *ospF* that exist independently of each other. We refer to this group of UHB-flanked genes collectively as the UHB gene family. The evolutionary relationships among UHB gene family members were assessed through DNA sequence analysis and gene tree construction. These analyses suggest that some UHB-flanked genes might actually represent divergent forms of other previously described genes. Analysis of the restriction fragment length polymorphism patterns of the UHB-flanked genes among *B. burgdorferi* isolates demonstrated that these patterns are highly variable among isolates, suggesting that these genes are not phylogenetically conserved. The variable restriction fragment length polymorphism patterns could indicate recombinational activity in these sequences. The presence of numerous copies of the UHB elements and the high degree of homology among UHB-flanked genes could provide the necessary elements to allow for homologous recombination, leading to the generation of recombination variants of UHB gene family members.

Several outer surface proteins (Osp) in the Lyme disease spirochetes have been characterized (6, 16, 20, 31, 42). Although the functions of the Osp have not yet been completely delineated, data suggest that they may play a role in spirochete-host interactions (10, 36). The Osp are being investigated as potential candidates for use in the development of Lyme disease vaccines (13–15). However, in view of the genetic diversity of these proteins and their variable expression, it is unclear if they will prove to be suitable targets (1, 12, 17, 24, 26, 27, 29, 31, 34, 37, 41, 43, 44). Several studies have also demonstrated that some *osp* genes undergo recombination at a relatively high frequency, which could suggest that these targets are insufficiently stable (27, 35). The phylogenetic diversity of the Lyme disease spirochetes is also an important factor to consider in vaccine and diagnostic assay development and has only recently been appreciated. *Borrelia burgdorferi*, originally identified as the single causative agent of Lyme disease (8), has been subdivided into several *Borrelia* species, including *B. burgdorferi*, *B. garinii*, *B. afzelii* (2, 7, 22, 23, 33, 42), *B. japonica* (18, 25, 32), and *B. andersonii* sp. nov. (25). To date, only *B. burgdorferi*, *B. garinii*, and *B. afzelii* have been clearly demonstrated to elicit disease in humans.

Two outer surface proteins, OspE and OspF, have recently been characterized (20), and their genes have been mapped to a circular plasmid of approximately 32 kb (1). These *osp* genes have been demonstrated to be highly immunogenic, and it has been suggested that they could be useful as vaccinogens (30). However, it remains to be determined whether these genes are sufficiently conserved, expressed, and universal among Lyme disease spirochetes isolates. Other circular-plasmid-carried genes that exhibit similarity with *ospEF* have been recently identified. These include *ospF* variants (1), *p21* (40), the *erp* genes (39), and *pG* (42). Expression of *ospEF* and related genes appears to be environmentally regulated to some degree, and some of these genes are expressed selectively during infection (1, 40, 42). It has been demonstrated that *ospEF* expression can be influenced by temperature; however, this effect is not consistent among isolates, and hence, a definitive correlation is not yet clear (38). Defining the distribution of specific genes, the factors that influence their expression, and the extent of their genetic and antigenic diversity is crucial in the development of effective vaccines and diagnostic assays.

We have characterized several genes from six *B. burgdorferi* isolates that are related to *ospE* and *ospF* and that comprise a gene family. A common feature of these genes is that they are each flanked at the 5′ end by a highly conserved upstream sequence. We have termed this conserved sequence the upstream homology box (UHB) and refer to this group of UHB-flanked genes as the UHB gene family. The UHB element, originally identified 5′ of the *ospEF* operon in *B. burgdorferi* N40, was found to occur in a variable number of copies among isolates. The observation that not all isolates carry the same total number of UHB elements suggests that not all isolates carry the same complement of UHB-flanked genes. In fact, some isolates were found to lack the *ospEF* operon. In some isolates, UHB-elements were found to flank *ospE* and *ospF* genes that exist independently of each other rather than as an operon as originally described for N40. To differentiate between *ospE* and *ospF* genes that exist in these different organizations, we have designated those not in an *ospEF* operon as *ospEi* and *ospFi* to indicate that they exist independently of each other. Comparative analysis of the UHB-flanked genes, *pG*, *bbk2.10*, the *erp* genes, *p21*, *ospE*, and *ospF* suggests that some of these genes might represent divergent forms of one another that have been modified through mutational events and genetic recombination. In fact, many of these gene designations could in fact be synonyms for the same gene. The identification of variant forms of the *ospEF* operon and related genes has important implications regarding the potential functional roles of the UHB gene family members, the interpretation of earlier data relating to the immune responses to these proteins, and the potential utility of these proteins in the development of Lyme disease-vaccines or diagnostic assays. In addition, recombination in and among members of this variable family of genes could provide a mechanism for the Lyme disease spirochetes to vary their antigenic profile and perhaps evade the mammalian immune response and maintain chronic infection.

MATERIALS AND METHODS

Bacterial cultivation and DNA and RNA isolation. The biological source and geographic origin of all *B. burgdorferi* isolates investigated are as follows: N40, cloned *Ixodes scapularis* tick isolate from New York (passaged through mice; infectious); N40CH, same as N40 but uncloned; B31, uncloned *I. scapularis* isolate from New York (infectious); CA12, uncloned *Ixodes pacificus* isolate from California (has not been tested for infectivity); 297, uncloned human cerebral spinal fluid isolate from a patient in Connecticut (infectious); and 297CH, same as 297 but passaged through hamsters (infectious). Isolates were cultivated in BSK-H medium (Sigma) supplemented with 6% rabbit serum (Sigma) at 32°C and harvested by centrifugation in a Beckman SA600 rotor spun at 8,000 rpm for 15 min. Cell pellets were washed with phosphate-buffered saline and repelleted. DNA and RNA were isolated from 50-ml cultures as previously described (26, 28).

PCR. PCR amplification was performed with *Taq* polymerase (Promega) as previously described (27). Cycling was performed with an MJ Research PTC100 thermal cycler. Primers were designed on the basis of the *B. burgdorferi* N40 *ospEF* sequence. Primer sequences are listed in Table 1. PCR volumes ranged from 25 to 50 μl, and 5 to 40 ng of template DNA was used. The reaction mixtures were overlaid with light mineral oil (CVS Pharmacy). PCR cycling conditions were as follows: 10 cycles of 94°C for 1 min, 50°C for 1 min, and 72°C for 1.5 min followed by 20 cycles of 94°C for 45 s, 50°C for 1 min, and 72°C for 1.5 min. To analyze the PCR products, 10 μl of each PCR mixture was subjected to agarose gel electrophoresis in either 1% GTG (United States Biochemical)–or 2% NuSieve 3:1 (FMC)–agarose gels in TAE buffer (27).

Cloning of PCR products. Freshly generated PCR products, purified with Wizard columns (Promega), were cloned into the pCR2.1 vector with the TA cloning kit as described by the supplier (Invitrogen). Recombinants carrying the desired inserts were identified by PCR colony screening. Briefly, colonies were picked with a sterile toothpick and touched to the surface of a new Luria-Bertani plate to generate a replica plate and then the remaining cells were resuspended in 50 μl of water. The cell suspension was boiled for 10 min and centrifuged at 13,000 × *g* for 10 s to remove cellular debris, and then 5-μl aliquots were used as templates in PCRs. The primers used to generate the original PCR product were used to screen the cell lysates. Reaction volumes were 50 μl, and PCR was performed and the amplicons were analyzed as described above.

Southern blot hybridizations. DNA was digested with *HaeIII* by standard methods, fractionated in 1.0% GTG–agarose gels, stained with ethidium bromide, and transferred onto Hybond N membranes (Amersham) with the XL VacuGene system (Pharmacia). The DNA was fixed to the membrane by UV cross-linking with the GS GeneLinker as instructed by the manufacturer (Bio-Rad). For Southern blot analysis, the membranes were incubated for 5 to 30 min in hybridization solution (27) and then overnight in the same solution with radioactively labeled oligonucleotide (15 ng/ml) or PCR-generated probes. Oligonucleotides were labeled at their 5′ OH groups with polynucleotide kinase and [γ-^{32}P]ATP, and PCR-generated probes were labeled by the high-prime method as instructed by the manufacturer (Boehringer Mannheim). To ensure that the PCR-generated probes were free of chromosomal DNA, a 20-fold diluted aliquot of a first-round PCR product was used as the template in a second round of PCR. The second-round products were purified with the Wizard column system (Promega), labeled, and used as probes. Hybridizations with oligonucleotide probes were conducted at 32°C, and those with PCR-generated probes were conducted at 45°C. Two 10-min washes with 2× SSC (1× SSC is 0.15 M NaCl plus 0.015 M sodium citrate)–0.1% sodium dodecyl sulfate (SDS) and one wash for 1 h with 0.2× SSC–0.1% SDS were performed. All washes were conducted at the temperature of hybridization.

DNA sequencing and sequence analyses. Either the sequencing templates were generated by TA cloning of PCR products as described above or the PCR products were purified with the Wizard system (Promega) and directly sequenced. Sequencing was accomplished with end-labeled primers and the *fmol* cycle sequencing system (Promega) according to the manufacturer's protocol. Sequencing reaction mixtures were electrophoresed in 6% agarose–8 M urea gels, and after electrophoresis the gels were transferred directly onto Whatman 3MM paper (without drying or treatment), covered with plastic wrap, and exposed to film with intensifying screens for 2 to 12 h.

DNA, amino acid sequence, and evolutionary analyses were conducted by using the Wisconsin Genetics Computer Group sequence analysis package (11). Sequences were aligned by using the PILEUP program, and evolutionary distances were determined by using the DISTANCE program. Distance values were then used to construct a gene or evolutionary tree by using the GROWTREE program. Distance values were also converted to identity values. The GAP program was used to determine pairwise percent sequence similarity values. Unless otherwise indicated, default values were used in all analyses.

Western blot (immunoblot) analysis of OspE and ospF expression. Pelleted cell cultures were resuspended in SDS solubilizing solution (100 μl for each unit of optical density at 640 nm of cells) and boiled for 10 min. The cell lysates were fractionated in SDS–12.5% polyacrylamide gels with a 4% stacking gel. The fractionated proteins were transferred onto immobilon-P membranes by electroblotting as previously described (24). The membranes were screened with antisera to OspF (two different preparations), OspE, and glutathione *S*-transferase. Anti-OspF antisera were generated with glutathione *S*-transferase-OspF fusion proteins originally cloned from two *B. burgdorferi* N40 cultures maintained in two different laboratories (1, 20). Anti-OspE antiserum was generated with a glutathione *S*-transferase-OspE fusion protein originally cloned from *B. burgdorferi* N40. The anti-OspF antiserum designated anti-OspF-AR was kindly provided by Darrin Akins and Justin Radolf, and the anti-OspF antiserum designated anti-OspF-LF, as well as the Anti-OspE antiserum, was provided by Tuan Lam and Erol Fikrig. The methods employed in immunoblot analysis were as previously described (1, 20).

Nucleotide sequence accession numbers. The sequence accession numbers (in parentheses) for all sequences analyzed in this report are as follows: N40 *ospE*

TABLE 1. Oligonucleotide sequences and target sites

Primer[a]	Sequence (5′ to 3′)	Target site[b]
uhb(+)	GTTGGTTAAAATTACATTTGCG	−128 to −107 of the *ospEF* UHB element
e13(+)	ATGTTTATTATTTGTGCTGTTT	13 to 40 of *ospE*
e46(+)	CTTATAGGTGCTTGCAAG	46 to 63 of *ospE*
e70(+)	ACTTCATATGATGAGCAAAGT	70 to 90 of *ospE*
e46(−)	CTTGCAAGCACCTATAAG	46 to 63 of *ospE*
e310(−)	AAACTAGTTTTAAATGATCC	310 to 327 of *ospE*
e470(−)	CTAGTGATATTGCATATTCAG	470 to 490 of *ospE*
f276(−)	ATATGTTTCAAGAGAAGTTT	276 to 295 of *ospF*
f414(−)	CTTAGCATCTTCTAAAGCTT	414 to 433 of *ospF*
f583(−)	CAATTCATTGCTATCAGTACC	583 to 606 of *ospF*
f634(−)	TTAAGCTCTTCATCAATCT	634 to 653 of *ospF*
f748(−)	AGAATGTATAAATAAACAAC	748 to 767 of *ospF*
p21-105(−)	CGCCATTGCTTTGCTTAACT	105 to 124 of *p21*
bapA489 (−)	CTAATCTTTGGGCAAATCAGC	489 to 509 of *bapA*

[a] The designations e and f indicate that the primers target *ospE* and *ospF*, respectively. The designations (+) and (−) indicate that the primers are plus-strand and negative-strand primers, respectively. The sequence of a minus-strand primer is the inverse complement of the coding sequence of the gene sequence.
[b] Primer numbering is based on the *B. burgdorferi* N40 *ospEF* sequence (20).

* Corresponding author. Mailing address: Department of Microbiology and Immunology, Room 7048-Sanger Hall, 1101 E. Marshall St., Richmond, VA 23298-0678. Phone: (804) 828-3779. Fax: (804) 828-9946. Electronic mail address: RMARCONI@GEMS.VCU.EDU.

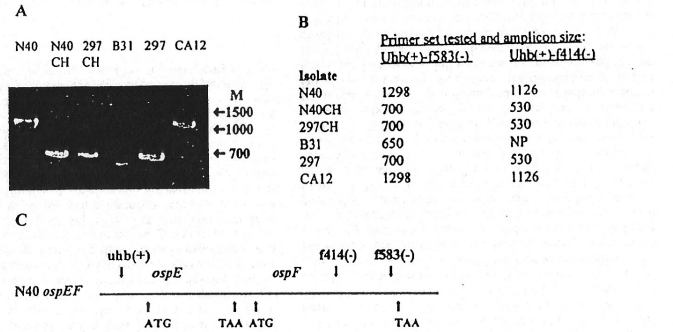

FIG. 1. PCR analysis of the *ospEF* operon. (A) PCR products obtained with the uhb(+)-f583(−) primer set. PCR was performed as described in the text. Molecular weight standards (M) are indicated to the right (in base pairs). The isolates tested are indicated above each lane. (B) The estimated amplicon sizes (in base pairs) obtained with the uhb(+)-f583(−) and uhb(+)-f414(−) primer sets are listed. NP, no product obtained. (C) A schematic representation of the PCR primer binding sites in *ospEF* from *B. burgdorferi* N40 is provided. The relative locations of primer binding sites are indicated by the arrows. Translational start and stop codons are indicated by ATG and TAA, respectively.

(L13924), N40 *ospF* (L13925), ZS7 *pG* and ZS7 *bapA* (X82409). N40 *p21* (L32797), 297 *bbk2.11* (U30617), 297 *bbk2.10* (U18292), N40 *bbk2.10* (U19105), 297 *ospF* (U19754), 297CH *ospEi* (L78245), 297CH *ospFi* (L78245), CA12 *ospEF* (L79960), N40CH *ospEi* (L78250), N40CH *ospFi* (L78251), and B31 *ospEi* (L78248).

RESULTS

PCR analyses of the *ospEF* operon. The e46(+)-f583(−) primer set, designed to amplify a segment of the *ospEF* operon extending from the 5′ end of *ospE* to the 3′ end of *ospF*, yielded a PCR product from *B. burgdorferi* N40 only. The N40-derived amplicon was 1,100 bp, consistent with that predicted by the published N40 *ospEF* sequence. Amplification of *ospEF* did not occur with B31 (the *B. burgdorferi* type strain), N40CH, CA12, 297, or 297CH. A 16S rRNA positive control primer set yielded products from all isolates, demonstrating that the failure to amplify *ospEF* was not due to template degradation or to the presence of PCR inhibitors (data not shown). To determine if the operon was absent or if sequence divergence within the primer binding sites prevented amplification, additional primer sets composed of the *ospF* minus-strand primers and various *ospE*-targeting plus-strand primers were tested. With most primer sets, product was obtained from isolate N40 only. However, the uhb(+) f583(−) primer set yielded products from all isolates (Fig. 1). The uhb(+) primer hybridizes upstream of the *ospEF* operon. While isolates CA12 and N40 yielded products of the expected size (1,300 bp), the amplicons from 297, 297CH, B31, and N40CH were several hundred base pairs smaller than expected. Consistent with this, the uhb(+)-f414(−) primer set also yielded truncated amplicons from 297, 297CH, and N40CH. Isolate B31 was not amplified with this primer set. The observed truncated amplicons and the failure to amplify the *ospEF* operon with several (+) primers that hybridize within *ospE* suggest that *ospE* might be absent or that *ospE* and *ospF* are not organized as an operon in all isolates.

DNA sequence analysis of PCR amplicons. (i) Sequence analysis of the N40, N40CH, 297CH, and 297 amplicons. To identify the molecular basis for the observed amplicon polymorphisms, the uhb(+)-f583(−)-generated amplicons were sequenced. In addition, the N40 *ospEF* amplicon was sequenced to determine if the organization and sequence of the *ospEF* operon carried by the N40 isolate used in our laboratory is the same as that described by Lam et al. (20). These sequences were found to be 100% identical. The N40CH and 297CH amplicon sequences are 98% identical to each other and exhibit high-level homology with *ospF* (1). The N40CH sequence was aligned with other *ospF*-related sequences (Fig. 2), and identity values among *ospF*-related sequences were determined (Table 2). Only a partial sequence for the amplicon from isolate 297 was determined; hence, this isolate was not subjected to further comparative sequence analysis. Over the regions for which the sequence was determined, the 297 amplicon sequence differed at only a few nucleotide positions from the 297CH and N40CH amplicon sequences. Each of these sequences carries a region of high-level identity (82%) to the upstream region of the *ospEF* operon, but they are not flanked by *ospE* and therefore are not part of an *ospEF* operon. Interestingly, the first 42 nucleotides of these independent *ospF* sequences exhibit higher identity values with the corresponding region from the N40 *ospE* (95%) than they do with the N40 *ospF* sequence (57%). Alignment of these independent *ospF* sequences with the full-length N40 *ospEF* operon sequence introduced a gap of 531 bp into the N40CH, 297, and 297CH sequences extending from position +43 of the N40 *ospE* through the intergenic spacer to position 36 of the N40 *ospF*. It is possible that these independent *ospF* sequences were generated by a deletion in *ospEF*, resulting in the formation of an in-frame chimeric *ospE-ospF* gene. We have designated this distinct form of *ospF* as *ospFi* to indicate that it is not part of an *ospEF* operon.

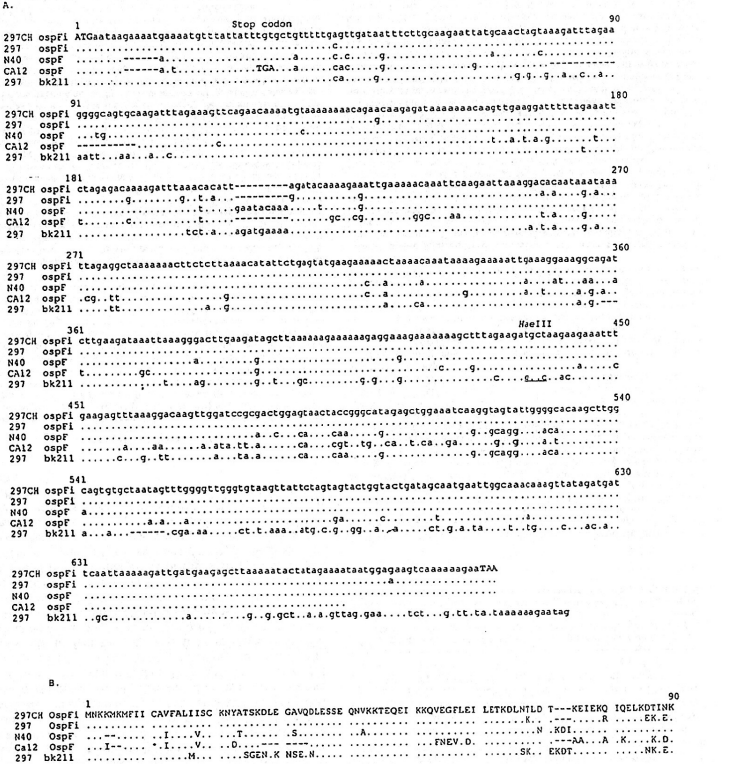

FIG. 2. Alignment of *ospF*-related sequences. The nucleotide sequence alignment (A) and the deduced amino acid sequences (B) are presented. Gaps introduced by alignment are indicated by hyphens, and identical positions are indicated by periods. The translational start and stop codons are indicated by boldface capital letters. Unique *HaeIII* sites are indicated in the nucleotide alignment. The premature stop codon present in the CA12 *ospF* sequence is underlined. The positions of stop codons in the amino acid alignments are indicated by asterisks. Blank spaces indicate positions at which the sequence was not determined. The identity of each gene sequence and its isolate of origin are indicated on the left. Note that all numbering of primers in this report is based on the numbering assigned to the continuous (i.e., nongapped) N40 sequence of the *ospEF* operon (20) and not the numbering, which includes gaps, in the alignment shown in this figure.

TABLE 2. Pairwise sequence comparisons for *ospF*-related sequences

Isolate and gene	% Identity[a]					
	297 *ospFi*	N40 *ospF*	N40CH *ospFi*	297CH *ospFi*	CA12 *ospF*	297 *bbk2.11*
297 *ospFi*		92	98	98	84	77
N40 *ospF*	87		91	93	84	78
N40CH *ospFi*	ND[b]	ND		96	84	78
297CH *ospFi*	97	89	ND		84	77
CA12 *ospF*	71	72	ND	71		72
297 *bbk2.11*	62	64	ND	61	47	

[a] The upper right half of the table lists the nucleotide identity values, and the lower left half provides the amino acid identity values.
[b] ND, not determined.

Through the use of additional primers, the 3′ region of *ospFi* from 297CH was amplified and the location of the translational stop codon was identified. *ospFi* encodes a polypeptide of 229 amino acids with a molecular mass of ~25,650 kDa. The N40 *ospF* sequence carries a 9-bp insertion approximately 205 bp into its coding sequence that is not present in *ospFi*. An insertion occurs at the analogous position in the *ospF* homolog, *bbk2.11* (1). Amino acid similarity values for *ospF*-related sequences are presented in Table 2, and the nucleotide and deduced amino acid sequences are presented in Fig. 2.

(ii) Sequence analysis of the *ospEF*-derived amplicons from isolates CA12 and B31. The CA12 derived uhb(+)-f583(−) amplicon is equivalent in size to the N40 *ospEF* amplicon, suggesting that this isolate carries an *ospEF* operon. However, since some primer sets were ineffective for amplifying *ospEF* from CA12 there might be sequence divergence between these operons. Sequence analysis of the operon from CA12 revealed this to be the case. Variability in the 5′ end of the coding sequence of *ospE* accounts for the negative amplification results obtained with several *ospE* plus-strand primers. At the nucleotide level, the CA12 and N40 *ospE* and *ospF* sequences are 83 and 86% identical, respectively. The *ospE* and *ospF* portions of the CA12 *ospEF* operon were aligned separately with related sequences in Fig. 2 and 4, respectively. Analysis of the CA12 *ospF* sequence revealed both a 21-bp deletion and a premature stop codon near the 5′ end of *ospF* (Fig. 2). The presence of the stop codon was confirmed by sequencing both strands of several independently generated PCR sequencing templates. The predicted molecular mass of the CA12 *ospE* polypeptide is 18,217 kDa.

Partial sequence analysis of the amplicon derived from isolate B31 and a subsequent BLAST search revealed that this sequence is nearly identical to the *B. burgdorferi* ZS7 *pG* sequence (42). The ZS7 sequence differs only by the presence of a 6-bp insertion. Amplification of *pG* with *ospEF*-directed primers reveals that there are regions of similarity among these genes.

PCR analyses of *ospE*: demonstration of independent *ospE* or *ospEi* genes and *ospE* variants. The analyses described above demonstrate that *ospFi* genes are carried by some isolates. To determine if isolates carrying *ospFi* also carry independent *ospE* genes or *ospEi*, PCR analyses using a minus-strand primer targeting the 3′ end of *ospE* and several different plus-strand primers that target upstream of *ospE* or the 5′ end of its coding sequence were performed. As described above, the *ospE* plus-strand primers did not yield products from isolates 297, 297CH, N40CH, and B31 when used with minus-strand primers targeting *ospF*. However, by using e470(−) primer and the same *ospE* plus-strand primers, products were obtained (Fig. 3). Consistent with the sequence analyses that demonstrated divergence in the e46(+) binding site in CA12, the e46(+)-e470(−) primer set did not yield a product with isolate CA12. While isolate N40 yielded the appropriately sized product with each primer set, some isolates yielded amplicons slightly larger than expected. Isolate N40CH yielded an amplicon slightly larger than expected, indicating that this isolate may harbor an insertion in its *ospE* gene. Isolate 297 yielded amplicons approximately 80 and 180 bp larger than the N40-derived amplicon. These analyses demonstrate the presence of polymorphisms in *ospEi* genes in some isolates.

Sequence analysis of *ospE*-derived amplicons. To determine the basis of the molecular polymorphisms in the *ospE*-derived amplicons and to assess the genetic variability within *ospE* among isolates, the uhb(+)-e470(−) amplicons were sequenced (Fig. 4). As predicted from the *ospE* PCR analyses, an insertion of 39 bp is present in the 5′ end of the N40CH *ospEi* gene. Sequence analysis also revealed that the multiple PCR products obtained from isolate 297 were due to the presence of repeats of some of the forward-primer binding sites within the 5′ end of *ospE* and were not due to the presence of multiple variants in the genome. Analysis of the upstream region of these amplicons revealed that the *ospEi* genes are also flanked by conserved UHB elements (discussed below and presented in Fig. 5). Sequence identity values were determined for *ospE*-related sequences and are presented in Table 3. Interestingly, the *ospEi* sequences are as closely related to N40 *p21* as they are to N40 *ospE*. Hence, the designation of genes with these sequences as *ospE* rather than *p21* is somewhat arbitrary. Since *ospE* was described first, we have opted for this nomenclature. Another interesting observation came from the analysis of the sequences downstream of the translational stop codons of the N40 *p21* (40) and *ospE* (20) genes. In isolate N40, the *ospE* gene resides 5′ of *ospF* and exists in an operon with the two genes separated by a short spacer. Alignment revealed that the first-80 bases 3′ of the translational stop codons of *ospE* and *p21* are 88% identical, indicating that a portion of the *p21* downstream sequence is homologous to the 5′ end of *ospF*. The *p21* sequence 3′ of this 80-base segment exhibits no strong homology with *ospF*. This observation could indicate that *p21* arose via a recombination event in an *ospEF* operon.

Identification of a shared and highly conserved upstream sequence common to several different related genes. All of the amplicons analyzed in this study carry the conserved UHB sequence element 5′ of their translational start codon. UHB sequences were aligned and are presented in Fig. 5. UHB elements have been demonstrated to flank *ospEF* (20), *pG* (42), *ospF*, *bbk2.10* (1), the *erp* genes (39), *p21* (19), and, as demonstrated in this report, *ospEi* and *ospFi*. The identity values for this sequence range from 81 to 100%. The central portion of the UHB element is nearly perfectly conserved among different UHB gene family members and among different *B. burgdorferi* isolates, which may suggest a potentially important role for this region in the transcriptional regulation of UHB-flanked genes. The UHB element contains a putative consensus ribosomal binding site and potential −10 sequence elements.

Evolutionary analyses of UHB-flanked genes. To compare the genetic relationships among UHB-flanked genes, the coding sequences determined here and those of other UHB-flanked genes were used to construct a gene, or evolutionary, tree (Fig. 6). These analyses demonstrate the close relationship of genes that have been considered to be distinct genes. For example, *ospE* and *p21* were found to cluster, and *pG* clustered with *bbk2.10*. *bapA* clustered with the *eppA* gene, which is carried on a 9.0-kb circular plasmid in *B. burgdorferi* B31 and which, like *pG*, has been demonstrated to be expressed only during infection (9). The evolutionary distances and clustering relationships indicate that some UHB-flanked genes are moderately divergent forms of each other rather than distinct genes.

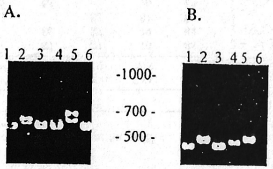

C.

Isolate	Primer set: uhb+/ e470-	e13+/ e470-	e46+/ e470-	e70+/ e470-	e46+/ f414-	e46+/ f583-
N40	620	480	450	420	910	1092
N40CH	670	530	500	470	NP	NP
B31	620	480	450	420	NP	NP
297CH	620	520	490	460	NP	NP
297	720-670	530	500	470	NP	NP
CA12	620	480	NP	420	NP	NP

D.

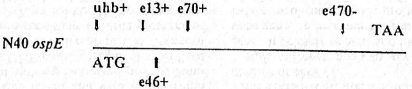

FIG. 3. PCR analyses of *ospE*. PCR analyses were performed as described in the text. Representative PCR results obtained with the uhb(+)-e470(−) (A) and e46(+)-e470(−) (B) primer sets are shown. A 10-μl aliquot of each PCR mixture was fractionated in a 1.0% agarose gel. The products obtained from isolates N40, N40CH, B31, 297CH, 297, and CA12 were loaded in lanes 1 through 6, respectively. (C) Additional *ospE* PCR results are summarized. The numbers indicate the estimated sizes of the amplicons in base pairs. NP, no product obtained. (D) Depiction of the relative binding sites of *ospE*-targeting oligonucleotides as they exist on the *ospE* gene of N40.

Southern blot hybridization analysis of UHB-flanked genes. To determine the number of UHB elements carried by each isolate, *Hae*III-digested DNA was probed with the uhb(+) oligonucleotide. The UHB copy number and the UHB restriction fragment length polymorphism (RFLP) patterns varied among isolates, with no two isolates yielding the same UHB RFLP pattern (Fig. 7A). Six hybridizing restriction fragments in N40 and 297, four in CA12, and two in B31, 297CH, and N40CH were observed. The intensity of the autoradiographic signal associated with each hybridizing band varied and could indicate that multiple UHB copies are carried on some restriction fragments. Alternatively, sequence variation in the uhb(+) probe binding site or the comigration of similarly sized fragments could be factors leading to differing hybridization intensities. Thus, some isolates could carry more UHB elements than indicated above. The detection of multiple hybridizing bands in the isogeneic isolate N40 is important, because it demonstrates that the UHB is in fact repeated in the genome and that we are not detecting different clonal variants in the population, each of which might carry only a single but variable copy of the UHB element. The observation that each isolate carries a different number of uhb(+)-hybridizing fragments suggests that each isolate does not carry the same complement of UHB-flanked genes.

To assess intraspecies variation in the organization of *ospE*, *ospF*, and related genes, RFLP pattern analyses using oligonucleotides targeting these genes were performed. Representative Southern blot data are presented in Fig. 7. Isolates N40 and CA12 were both found by PCR to carry *ospEF*, and as expected, all *ospE* and *ospF* probes tested hybridized with a single fragment (5.5 kb) in isolate N40 and a single fragment (4.4 kb) in isolate CA12. The uhb(+) probe however did not hybridize with the 4.5-kb fragment from CA12. This is consistent with the DNA sequence analyses that revealed a *Hae*III site within the *ospE* gene that would place the UHB element on a separate *Hae*III restriction fragment. It is noteworthy that some *ospE* and *ospF* oligonucleotide probes hybridized with more than one restriction fragment, indicating that some regions of *ospE* and *ospF* are repeated in the genomes of some isolates (Fig. 7B to D). The identities of these hybridizing sequence elements are unclear, but they could represent other members of the UHB gene family that have not yet been characterized.

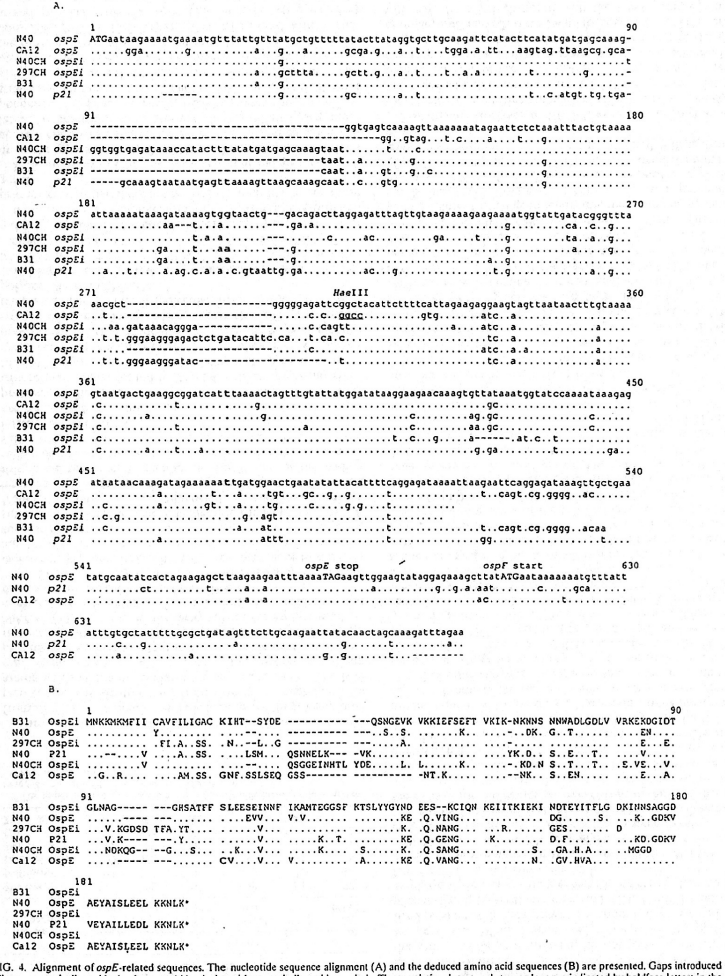

FIG. 4. Alignment of *ospE*-related sequences. The nucleotide sequence alignment (A) and the deduced amino acid sequences (B) are presented. Gaps introduced by alignment are indicated by hyphens, and identical positions are indicated by periods. The translational start and stop codons are indicated by boldface letters in the nucleotide alignments and by asterisks in the amino acid alignments. Blank spaces indicate positions at which the sequence was not determined. The identity of each gene sequence and its isolate of origin are indicated on the left. Note that all numbering of primers in this report is based on the numbering assigned to the continuous (i.e., nongapped) N40 sequence of the *ospEF* operon (20) and not the numbering, which includes gaps, in the alignment shown in this figure.

FIG. 5. Alignment of the UHBs from different UHB gene family members from different *B. burgdorferi* isolates. Hyphens indicate gaps, periods indicate identical positions, and blank spaces indicate positions at which the sequence was not determined. The putative start codon and ribosomal binding site (RBS) of the associated coding sequence are indicated in boldface type and are labeled above the sequence.

Hybridization patterns consistent with the presence of either *ospEi* or *ospFi* were also observed. For example, in isolate B31 a 1.5-kb UHB-positive fragment hybridized with all *ospE*-targeting oligonucleotide probes tested and with a full-length *ospE* PCR product but not with *ospF*-directed probes. Similarly, in isolate 297 a 2.1-kb UHB-positive fragment hybridized with all *ospE* probes tested but not with *ospF* probes. Southern analyses also provided results consistent with the presence of *ospFi* in some isolates. In 297, an 8.6-kb UHB-positive fragment hybridized with the f414(−) and f583(−) *ospF* probes, consistent with the presence of *ospFi* rather than *ospEF*. In an earlier report, Akins et al. also demonstrated the existence of an *ospFi* gene in isolate 297 (1).

Results not predicted by PCR analyses were also observed. For example, the f414(−) oligonucleotide hybridized with three different UHB-positive fragments in isolate 297 (Fig. 7B), yet in the PCR analyses described above, only one uhb(+)-f414(−)-derived amplification product was observed. One of the three f414(−)-hybridizing fragments also bound the f583(−) oligonucleotide, suggesting that this fragment carries *ospFi*. Failure to amplify the additional elements with the uhb(+)-f414(−) primer set could be due to a wide variety of reasons. The identities of the sequence elements that bound these probes are unclear, but they may represent other UHB gene family member genes that show homology with *ospF*. Two such variants, *bbk2.10* and *bbk2.11*, have been described previously (1). However, since the only potential f414(−) binding sites in these genes contain four mismatches with the f414(−) probe and the f414(−) probe binding site in *bbk2.11* contains a *Hae*III restriction site, it is unlikely that these fragments carry *bbk2.10* or *bbk2.11*.

TABLE 3. Pairwise sequence comparisons for *ospE*-related sequences

Isolate and gene	% Identity[a]					
	B31 *ospEi*	N40 *ospE*	297CH *ospEi*	N40CH *ospEi*	CA12 *ospE*	N40 *p21*
B31 *ospEi*		91	89	87	79	86
N40 *ospE*	81		86	87	79	84
297CH *ospEi*	82	72		82	81	86
N40CH *ospEi*	77	75	68		76	80
CA12 *ospE*	64	62	68	61		79
N40 *p21*	81	77	80	71	73	

[a] The upper right half of the table lists the nucleotide identity values, and the lower left half provides the amino acid identity values.

ospE sequence analyses revealed that the *p21* and *ospE* genes are closely related and likely are divergent forms of the same gene. To determine if copies of both are carried by each isolate, an oligonucleotide probe directed at a unique segment of *p21* was made and used in Southern analyses. In all isolates, the *p21* probe hybridized with a 2.0-kb fragment that did not bind the uhb(+) oligonucleotide, a 120-bp PCR-generated UHB probe (data not shown), or any of the *ospE*-directed probes. *Hae*III sites are not present in the N40 *p21* sequence previously determined by Suk et al. (40); hence, at least in isolate N40 the hybridization of both the *p21* and UHB-targeting probes with the same fragment was expected but not observed. It is unclear if this is due to sequence variations or genomic rearrangements in *p21*.

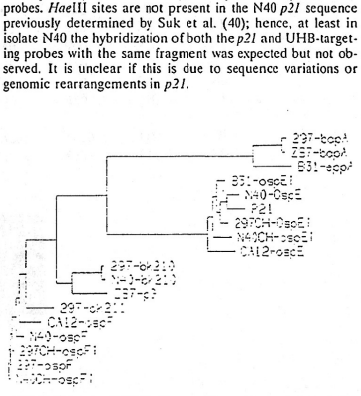

FIG. 6. Gene tree of UHB family genes. The gene tree was constructed on the basis of the coding sequence of each UHB gene family member as described in the text. The labeling indicates the gene identity and its isolate of origin. Sequence accession numbers can be found in the text.

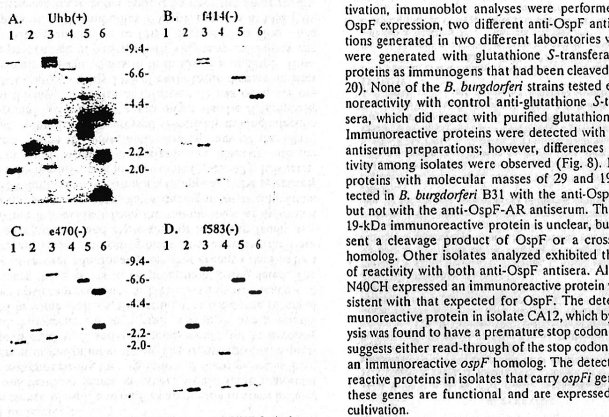

FIG. 7. RFLP pattern analysis of UHB elements and UHB-flanked genes. DNA was digested with *Hae*III, fractionated, and probed with oligonucleotide uhb(+) (A), f414(−) (B), e470(−) (C), or f583(−) (D). In each panel, restricted DNAs from isolates B31, 297CH, 297, N40CH, N40, and CA12 were loaded in lanes 1 through 6, respectively. Molecular weight markers are indicated in kilobases.

The isolates 297CH and N40CH are derivative populations of isolates 297 and N40, respectively. These isolates exhibited RFLP patterns different from those of 297 and N40 with all probes tested except the *p21* probe. This observation demonstrates that both the uncloned N40 and 297 isolates are, perhaps not surprisingly, composed of a mixed population of cell lineages. Isolates N40CH and 297CH carry only two UHB-positive fragments, suggesting that these isolates might not carry all of the known UHB-flanked genes. Some of the UHB-carrying fragments hybridized only weakly with the uhb(+) oligonucleotide, which could indicate sequence divergence in this repeated sequence in these isolates.

Immunoblot analysis of *ospE*, *ospF*, and other *ospEF* gene family variants. To determine if OspE, OspF, or other immunologically related proteins are expressed during in vitro cultivation, immunoblot analyses were performed. In assessing OspF expression, two different anti-OspF antiserum preparations generated in two different laboratories were used. Both were generated with glutathione *S*-transferase-OspF fusion proteins as immunogens that had been cleaved and purified (1, 20). None of the *B. burgdorferi* strains tested exhibited immunoreactivity with control anti-glutathione *S*-transferase antisera, which did react with purified glutathione *S*-transferase. Immunoreactive proteins were detected with both anti-OspF antiserum preparations; however, differences in immunoreactivity among isolates were observed (Fig. 8). Immunoreactive proteins with molecular masses of 29 and 19 kDa were detected in *B. burgdorferi* B31 with the anti-OspF-LF antiserum but not with the anti-OspF-AR antiserum. The identity of the 19-kDa immunoreactive protein is unclear, but it could represent a cleavage product of OspF or a cross-reactive OspF homolog. Other isolates analyzed exhibited the same pattern of reactivity with both anti-OspF antisera. All isolates except N40CH expressed an immunoreactive protein with a mass consistent with that expected for OspF. The detection of an immunoreactive protein in isolate CA12, which by sequence analysis was found to have a premature stop codon in its *ospF* gene, suggests either read-through of the stop codon or expression of an immunoreactive *ospF* homolog. The detection of immunoreactive proteins in isolates that carry *ospFi* genes suggests that these genes are functional and are expressed during in vitro cultivation.

In all isolates except B31, immunoblot analyses using anti-OspE (N40) antisera detected an immunoreactive protein with a molecular mass of approximately 34 kDa, considerably larger than the predicted 19-kDa OspE (Fig. 6). In B31, two proteins with molecular masses of approximately 19 and 31 kDa were detected with this antiserum. In addition to B31, polypeptides consistent with the size expected for OspE were observed (albeit faintly) in isolates N40, 297, and 297CH.

The immunoblot results presented here differ qualitatively from data recently presented by Stevenson et al. (39). These authors utilized the same anti-OspE and anti-OspF-LF antisera used in this study. Cross-reactivity of the anti-OspE antiserum with 43- and 68-kDa proteins in isolate B31 (38) was reported. This is in contrast to the approximately 34-kDa cross-reactive proteins observed in this study. Interestingly, in an earlier analysis Stevenson et al. detected a cross-reactive protein in isolate B31 with an apparent molecular mass of 35 kDa (38) and did not observe an immunoreactive protein with a molecular mass of 43 kDa as presented in their more recent analysis. It is unclear whether different proteins in different laboratories are being detected with this antiserum or whether the same immunoreactive proteins are being observed but there is a discrepancy in the estimated molecular masses. Differences were also observed with the anti-OspF-LF antiserum. Specifically, it was also reported previously that the anti-OspF-LF serum also recognizes the 43- and 68-kDa proteins that were immunoreactive with the anti-OspE antisera. In this study, we did not observe immunoreactivity of these proteins with either of the two independently generated anti-OspF antisera that were tested. These antisera did not detect the approximately 34-kDa proteins that were detected with the anti-OspE antiserum. The reasons for these discrepancies are currently unclear, but in spite of this, it is apparent from this and earlier studies that proteins immunologically related to OspE are expressed in vitro by *B. burgdorferi* and that OspE is apparently expressed at low levels and only in some isolates during in vitro cultivation.

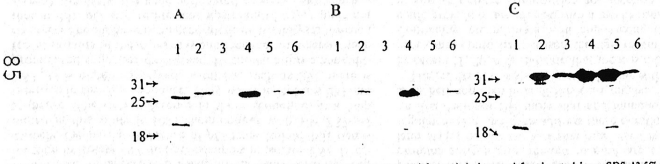

FIG. 8. Immunoblot analyses of OspE and OspF. Whole cell lysates were prepared for each isolate and fractionated in an SDS–12.5% polyacrylamide gel as described in the text. The proteins were transferred onto Immobilon-P membranes and screened with either OspF or OspE antiserum as described in the text. In lanes 1 through 6 of each panel, the following *B. burgdorferi* isolates were analyzed: B31, 297CH, N40CH, N40, CA12, and 297, respectively. The isolates were screened with anti-OspF-LF (A), anti-OspF-AR (B), or anti-OspE antiserum. The migration positions of the molecular mass markers (in kilodaltons) are indicated.

DISCUSSION

ospE and *ospF* were first cloned and sequenced from *B. burgdorferi* N40 (20), an isolate that has been widely used in Lyme disease-related research. These genes were found to be closely spaced, and hence it was suggested that they constitute an operon. The conservation, organization, and distribution of this operon among other *B. burgdorferi* isolates have not been previously assessed. Recently, other genes that exhibit homology with *ospF* or *ospE* and that are flanked by a UHB element have been identified (1, 20, 39, 40, 42). These include *p21*, *pG*, *erp* genes, *ospEi*, *ospFi*, and *bbk2.10*. Like *ospEF*, little is known about the organization, distribution, conservation, and biological role of the UHB-flanked genes. The purpose of this study was to begin to address these questions, as they pertain to the causative agent of Lyme disease in North America, *B. burgdorferi*.

PCR, Southern blot hybridization, and DNA sequence analyses demonstrated that not all isolates carry an *ospEF* operon analogous to that described for isolate N40 (20). Four of six isolates instead carry separate copies of *ospE* or *ospF*. To differentiate these genes from their counterparts, which are organized in an operon, the suffix "i" has been added to their designations to indicate that they exist independently of each other and carry their own promoter-containing UHB element. Recent analyses of other *B. burgdorferi* sensu lato isolates indicate that most isolates lack *ospEF* (21). Preliminary PCR analyses on 65 *B. burgdorferi* sensu lato isolates have demonstrated that only 8% carry an *ospEF* operon (21). Akins et al. had previously demonstrated the existence of *ospFi* genes in two *B. burgdorferi* isolates (1).

The RFLP patterns of *ospEF*, *ospEi*, *ospFi*, and other UHB-flanked genes were found to be highly variable. The RFLP patterns of other *B. burgdorferi* sensu lato genes tend to exhibit relatively species-specific or subspecies-specific patterns. There are exceptions, such as the *ospD* gene (27). The variable patterns of this gene have been suggested to result from recombination and lateral transfer of the *ospD* plasmid among isolates. These processes can result in RFLP patterns that are not reflective of the overall phylogenetic divergence of organisms. The analyses presented here demonstrate that the RFLP patterns of the UHB-flanked genes are hypervariable at the intraspecies level and thus, like *ospD*, are not indicative of phylogenetic relationships. This suggests that these genes have been influenced by short-term evolutionary or mutational events such as genetic recombination. A relatively high frequency of recombination would be required to result in what appear to be isolate-specific RFLP patterns.

Southern blot hybridization experiments have also demonstrated that regions of the coding sequence of some UHB-flanked genes are present in more than one copy in some isolates. This is consistent with results of studies by Akins et al., which also demonstrated that probes directed against various regions of *ospF* hybridize with more than one restriction fragment upon Southern blot analysis (1). These observations raise the possibility that there might be additional genes that are related to members of the UHB gene family that have not yet been identified. On the basis of the variable copy number of the UHB elements, it appears that the complement of UHB-flanked genes carried among isolates varies. It is conceivable that some UHB-flanked genes could have arisen via gene duplication events, as has been speculated for *ospA* and *ospB* (35), or that they represent recombination variants. Recombination in these genes is evident in the form of insertions and deletions. Several such polymorphisms were detected in both *ospEi* and *ospFi*. Recombination might have played a role in the generation of genes such as *ospFi*. We have noted that if the first 42 nucleotides of *ospFi*, *ospE*, and *ospF* are aligned without gaps then *ospFi* exhibits a level of identity with *ospE* significantly higher than that with *ospF* (95 versus 57%). In addition, *ospFi* also carries the same upstream sequence as *ospEF*. This observation and the absence of a full-length *ospEF* operon suggest that *ospFi* arose through a deletion or recombination event in *ospEF*, with the outcome of this deletion being the fusion of partial *ospE* and *ospF* genes to form a chimeric gene. Alternatively, it is possible that *ospEi* and *ospFi* represent the ancestral forms of these genes and that the *ospEF* operon arose from a recombination event.

Alignment of UHB-flanked gene sequences revealed that many have extended regions of homology. Hence, sequence-mediated recombination among these genes would not be unlikely and could represent a mechanism by which variability among these genes has been generated. If recombination and genetic rearrangement occur at high enough frequencies, the UHB copy numbers, organization, and polymorphisms in these genes could to some degree be lineage or even isolate specific. Monitoring of the stability of the organization of these genes in clonal populations over time will aid in assessing these possibilities.

The evolutionary analyses suggest that some previously characterized UHB-flanked genes might be divergent forms of one another. For example the *p21* and *ospE* genes from isolate N40 are 87% identical at the nucleotide level. At the amino acid level they exhibit 80% identity and 85% similarity. Similarly, the recently described *erpA* and *erpC* genes are also closely related to *ospE*, exhibiting identity values of 85 and 88% at the nucleotide level (39). Typically, sequences with identity values of this magnitude are considered to be variants of the same gene. Other examples are the *pG* and *bbk2.10* genes, which, upon gene tree construction, were found to cluster. Both are UHB-flanked genes that are selectively expressed during infection (1, 42). The *pG* and *bbk2.10* sequences are 77% identical at the nucleotide level. At the amino acid level they are 62% identical and 72% similar. Divergence among these sequences is most pronounced in their central portions. The first 41 amino acids of these proteins exhibit 80% identity. The last 51 amino acids also show 80% identity. It is possible that divergence in the central portion of *pG* could have arisen between two related genes through homologous recombination mediated by the homologous sequence elements at the 5′ and 3′ ends. The suggestion that *pG* and *bbk2.10* are derived from the same ancestral gene is supported by the fact that both are flanked by the same downstream sequence. In *B. burgdorferi* ZS7, *pG* resides immediately upstream of the *bapA* gene. The *bbk2.10* sequence reported by Akins et al. (1) resides just 5′ of a sequence with 98% nucleotide identity to that of *bapA*.

Hence *bbk2.10* appears to reside in the same relative map location in isolate 297 that *pG* occupies in isolate ZS7. Interestingly, the partial sequence of *pG* from isolate B31 determined in this study is 100% homologous with the ZS7 *pG* sequence. The only difference in these sequences is a 6-bp insertion in the ZS7 sequence. Thus, while in isolates B31 and ZS7 *pG* is highly conserved, in others, such as 297, there is pronounced sequence divergence. Recombination among different variants of these genes is one mechanism whereby such divergence could have been generated. PCR analyses revealed that in B31, *pG* also resides just upstream of *bapA* (data not shown). Similarly, the gene designated as *erpG* (39), which is nearly identical to *pG*, also resides 5′ of the *bapA* gene in some clones of isolate B31. It appears that *erpG*, *bbk2.10*, and *pG* are synonyms.

The *ospA*, *ospB*, and *ospC* genes have been extensively analyzed regarding intraspecies variability. For OspC, amino acid identity values have been found to range from 61 to 100% (41), and for OspA and OspB, they range from 69 to 100% (43). Thus, gene sequences that fall within this range of identity values are considered to be variants of the same gene and are designated as such. The range in identity values among genes such as *p21*, *erpA*, *erpC*, and *ospE* suggests that these genes are synonyms, exhibiting a degree of variability among isolates that is not unexpected. Hence, it remains to be determined if the designation of each gene as different is warranted. Likewise, the identities observed among *bbk2.10*, *erpG*, and *pG*, as well as that between *eppA* and *bapA*, are also indicative of these genes being synonymous. In light of this, a revision of the currently used nomenclature might be warranted and would serve to simplify the nomenclature of *Borrelia* genes. We have opted to utilize the first designations assigned to these genes, i.e., to refer to *p21*, *erpA*, and *erpC* as *ospE* (20) and to replace *bbk2.10* and *erpG* with *pG* (42). A final revised nomenclature might be possible once the extent of variability of the UHB gene family among *B. burgdorferi* sensu lato isolates as a whole is better understood.

The presence of *ospE* and *ospF* as an operon in some isolates and as independent genes in others would have important implications concerning the regulation of these genes in these two different organizational states. The transcriptional expression of individual *ospE* and *ospF* genes would not by necessity be linked. However, although *ospE* and *ospF* are physically separated in some isolates, they still share the same potential regulatory upstream sequence or UHB. As a consequence, one might expect these genes to be potentially coregulated. The existence of several additional genes that are also flanked by a UHB element raises interesting questions regarding the transcriptional regulation and expression of this gene family as a whole. While it is evident from the immunoblot analyses that *ospF* is expressed by most isolates during in vitro cultivation, other UHB-flanked genes are not and appear to be selectively expressed during infection in mammals (1, 40, 42). It is interesting that *eppA*, which shares significant identity with the *bapA* gene, which is immediately downstream of the UHB-flanked *pG* gene, is also expressed selectively during infection (9). Individual UHB-flanked genes might also be differentially regulated during the course of infection. It has been demonstrated that approximately 14% of early Lyme disease patients possess circulating antibodies to both OspE and OspF. However, the percentage of patients with long-term infections who have circulating antibodies to OspF increases to 58% while that for patients with antibodies to OspE remains at 14% (30). Hence, although these genes appear to have the same regulatory sequence, *ospFi* expression might be up regulated while expression of *ospEi* remains unchanged. Alternatively, it is possible that other UHB gene family members that encode proteins antigenically related to *ospF* are expressed during later stages of disease and that *ospF* itself is not actually up regulated. Our ability to address these questions requires that we first decipher the molecular and immunological relationships between members of this gene family.

The results of this study, in combination with data presented by others (1, 20, 42), indicate that there is a family of related genes that could have arisen through recombination events. Continuing recombination in and among these sequences could provide *B. burgdorferi* with a mechanism to rapidly alter its surface antigen composition and increase its antigenic diversity. This process could play a role in mediating the bacterium-host interaction postinfection and allow for the establishment of long-term infection in mammals. Similarly, antigenic variation among members of the Vmp protein family is a key factor in the pathogenesis of the relapsing fever borrelia (3). In the relapsing fever spirochetes, recombination in and among the *vmp* genes plays a key role in the generation of antigenic variants (3–5). Although the UHB-flanked genes are located on circular plasmids (1, 21, 39) in contrast to the *vmp* genes which are located on linear plasmids, it is tempting to speculate that there could be parallels between the biological role of the *vmp* gene family and the UHB gene family. Work to characterize UHB gene family members, the mechanisms by which they arise, and the factors or conditions that influence their transcription continues.

ACKNOWLEDGMENTS

We thank Chauna, Ryan, and Cherie for helpful discussions; Erol Fikrig for kindly providing anti-OspE, anti-OspF, and anti-glutathione *S*-transferase antisera; and Darrin Akins and Justin Radolf for kindly providing anti-*B. burgdorferi* 297 OspF antisera, for helpful discussions, and for sharing data prior to publication.

This work was supported in part by grants from the Jeffress Trust and the National Institutes of Health.

REFERENCES

1. Akins, D., S. F. Porcella, T. G. Popova, D. Shevchenko, S. I. Baker, M. Li, M. V. Norgard, and J. D. Radolf. 1995. Evidence for *in vivo* but not *in vitro* expression of a *Borrelia burgdorferi* outer surface protein F (OspF) homologue. Mol. Microbiol. 18:507–520.
2. Baranton, G., D. Postic, I. Saint Girons, P. Boerlin, J.-C. Piffaretti, M. Assous, and P. A. D. Grimont. 1992. Delineation of *Borrelia burgdorferi* sensu stricto, *Borrelia garinii* sp. nov., and group VS461 associated with Lyme borreliosis. Int. J. Syst. Bacteriol. 42:378–383.
3. Barbour, A. G. 1990. Antigenic variation of a relapsing fever *Borrelia* species. Annu. Rev. Microbiol. 44:155–171.
4. Barbour, A. G., N. Byrman, C. J. Carter, T. Kitten, and S. Berstrom. 1991. Variable antigen genes of the relapsing fever agent *Borrelia hermsii* are activated by promoter addition. Mol. Microbiol. 5:489–493.
5. Barbour, A. G., C. J. Carter, N. Burman, C. S. Freitag, C. F. Garon, and S. Bergstom. 1991. Tandem insertion sequence-like elements define the expression site for variable antigen genes of *Borrelia hermsii*. Infect. Immun. 59: 390–397.
6. Barbour, A. G., S. L. Tessier, and W. J. Todd. 1983. Lyme disease spirochetes and ixodid tick spirochetes share a common surface antigenic determinant defined by a spirochete *Borrelia burgdorferi*. Mol. Microbiol. 3:479–486.
7. Boerlin, P., O. Peter, A.-G. Bretz, D. Postic, G. Baranton, and J.-C. Piffaretti. 1992. Population genetic analysis of *Borrelia burgdorferi* isolates by multilocus enzyme electrophoresis. Infect. Immun. 60:1677–1683.
8. Burgdorfer, W., A. G. Barbour, S. F. Hayes, J. L. Benach, E. Grunwaldt, and J. P. Davis. 1982. Lyme disease—a tick-borne spirochetosis? Science 216: 1317–1319.
9. Champion, C. I., D. R. Blanco, J. T. Skare, D. A. Haake, M. Giladi, D. Foley, J. N. Miller, and M. A. Lovett. 1994. A 9.0-kilobase-pair circular plasmid of *Borrelia burgdorferi* encodes an exported protein: evidence for expression only during infection. Infect. Immun. 62:2653–2661.
10. Coleman, J. L., R. C. Rogers, and J. L. Benach. 1992. Selection of an escape variant of *Borrelia burgdorferi* by use of bactericidal monoclonal antibodies to OspB. Infect. Immun. 60:3098–3104.
11. Devereux, J., P. Haeberli, and O. Smithies. 1984. A comprehensive set of sequence analysis programs for the VAX. Nucleic Acids Res. 12:387–395.
12. Fikrig, E., H. Tao, F. S. Kantor, S. W. Barthold, and R. A. Flavell. 1993. Evasion of protective immunity by *Borrelia burgdorferi* by truncation of outer surface protein B. Proc. Natl. Acad. Sci. USA. 90:4092–4096.
13. Fikrig, E. F., S. W. Barthold, F. S. Kantor, and R. A. Flavell. 1990. Protection of mice against the Lyme disease agent by immunizing with recombinant OspA. Science 250:553–556.
14. Fikrig, E. F., S. W. Barthold, N. Marcantonio, K. Deponte, F. S. Kantor, and R. A. Flavell. 1992. Roles of OspA, OspB, and flagellin in protective immunity to Lyme borreliosis in laboratory mice. Infect. Immun. 59:553–559.
15. Fikrig, E. F., S. R. Telford, S. W. Barthold, F. S. Kantor, A. Spielman, and R. A. Flavell. 1992. Elimination of *Borrelia burgdorferi* from vector ticks feeding on OspA-immunized mice. Proc. Natl. Acad. Sci. USA 89:5418–5421.
16. Fuchs, R., S. Jauris, F. Lottspeich, V. Preac-Mursic, B. Wilske, and E. Soutschek. 1992. Molecular analysis and expression of a *Borrelia burgdorferi* gene encoding a 22 kDa protein (pC) in *Escherichia coli*. Mol. Microbiol. 6:503–509.
17. Jonsson, M., L. Noppa, A. G. Barbour, and S. Bergström. 1992. Heterogeneity of outer membrane proteins in *Borrelia burgdorferi*: comparison of *osp* operons of three isolates of different geographic origins. Infect. Immun. 60:1845–1853.
18. Kawabata, H., T. Masuzawa, and Y. Yanagihara. 1993. Genomic analysis of *Borrelia japonica* sp. nov. isolated from *Ixodes ovatus* in Japan. Microbiol. Immunol. 37:843–848.
19. Lam, T. L., T.-P. K. Nguyen, E. Fikrig, and R. A. Flavell. 1994. A chromosomal *Borrelia burgdorferi* gene encodes a 22-kilodalton lipoprotein, P22, that is serologically recognized in Lyme disease. J. Clin. Microbiol. 32:876–883.
20. Lam, T. T., T.-P. K. Nguyen, R. R. Montgomery, F. S. Kanter, E. Fikrig, and R. A. Flavell. 1994. Outer surface protein E and F of *Borrelia burgdorferi*, the agent of Lyme disease. Infect. Immun. 62:290–298.
21. Marconi, R. T. Unpublished data.
22. Marconi, R. T., and C. F. Garon. 1992. Identification of a third genomic group of *Borrelia burgdorferi* through signature nucleotide analysis and 16S rRNA sequence determination. J. Gen. Microbiol. 138:533–536.
23. Marconi, R. T., and C. F. Garon. 1992. Phylogenetic analysis of the genus *Borrelia*: a comparison of North American and European isolates of *B. burgdorferi*. J. Bacteriol. 174:241–244.
24. Marconi, R. T., M. E. Konkel, and C. F. Garon. 1993. Variability of *osp* genes and gene products among species of Lyme disease spirochetes. Infect. Immun. 61:2611–2617.
25. Marconi, R. T., D. Liveris, and I. Schwartz. 1995. Identification of novel insertion elements, restriction fragment length polymorphism patterns, and discontinuous 23S rRNA in Lyme disease spirochetes: phylogenetic analyses of rRNA genes and their intergenic spacers in *Borrelia japonica* sp. nov. and genomic group 21038 (*Borrelia andersonii* sp. nov.) isolates. J. Clin. Microbiol. 33:2427–2434.
26. Marconi, R. T., D. S. Samuels, and C. F. Garon. 1993. Transcriptional analyses and mapping of the *ospC* gene in Lyme disease spirochetes. J. Bacteriol. 175:926–932.
27. Marconi, R. T., D. S. Samuels, R. K. Landry, and C. F. Garon. 1994. Analysis of the distribution and molecular heterogeneity of the ospD gene among the Lyme disease spirochetes: evidence for lateral gene exchange. J. Bacteriol. 176:4572–4582.
28. Marconi, R. T., J. Wigboldus, H. Weissbach, and N. Brot. 1991. Transcriptional start site and MetR binding sites on the *Escherichia coli met* H gene. Biochem. Biophys. Res. Commun. 175:1057–1063.
29. Margolis, N., and P. A. Rosa. 1993. Regulation of expression of major outer surface proteins in *Borrelia burgdorferi*. Infect. Immun. 61:2207–2210.
30. Nguyen, T.-P. K., T. T. Lam, S. W. Barthold, S. R. Telford III, R. A. Flavell, and E. Fikrig. 1994. Partial destruction of *Borrelia burgdorferi* within ticks that engorged on OspE- or OspF-imnunized mice. Infect. Immun. 62:2079–2084.
31. Norris, S. J., C. J. Carter, J. K. Howell, and A. G. Barbour. 1992. Low-passage-associated proteins of *Borrelia burgdorferi* B31: characterization and molecular cloning of OspD, a surface-exposed, plasmid-encoded lipoprotein. Infect. Immun. 60:4662–4672.
32. Postic, D., J. Belfazia, E. Issgal, I. Saint Girons, P. A. D. Grimont, and G. Baranton. 1993. A new genomic species in *Borrelia burgdorferi sensu lato* isolated from Japanese ticks. Res. Microbiol. 144:467–473.
33. Postic, D., C. Edlinger, C. Richaud, F. Grimont, Y. Dufresne, P. Perolat, G. Baranton, and P. A. D. Grimont. 1990. Two genomic species in *Borrelia burgdorferi*. Res. Microbiol. 141:465–475.
34. Rosa, P. A., D. Hogan, and N. Margolis. 1992. Molecular analysis of the major outer surface protein locus from a divergent *Borrelia burgdorferi* isolate from Europe, p. 95–110. *In* S. E. Schutzer (ed.), Lyme disease: molecular and immunologic approaches. Cold Spring Harbor Laboratory Press, Cold Spring Harbor, N.Y.
35. Rosa, P. A., C. Schwan, and D. Hogan. 1992. Recombination between genes encoding major outer surface proteins A and B of *Borrelia burgdorferi*. Mol. Microbiol. 6:3031–3040.
36. Sadziene, A., A. G. Barbour, P. A. Rosa, and D. D. Thomas. 1993. An OspB mutant of *Borrelia burgdorferi* has reduced invasiveness in vitro and reduced infectivity in vivo. Infect. Immun. 61:3590–3596.
37. Schwan, T. G., J. Piesman, W. T. Golde, M. C. Dolan, and P. A. Rosa. 1995. Induction of an outer surface protein on *Borrelia burgdorferi* during tick feeding. Proc. Natl. Acad. Sci. USA 92:2909–2913.
38. Stevenson, B., T. G. Schwan, and P. Rosa. 1995. Temperature-related differential expression of antigens in the Lyme disease spirochete *Borrelia burgdorferi*. Infect. Immun. 63:4535–4539.
39. Stevenson, B., K. Tilly, and P. A. Rosa. 1996. A family of genes located on four separate 32-kilobase circular plasmids in *Borrelia burgdorferi* B31. J. Bacteriol. 178:3508–3516.
40. Suk, K., S. Das, W. Sun, B. Jwang, S. W. Barthold, R. A. Flavell, and E. Fikrig. 1995. *Borrelia burgdorferi* genes selectively expressed in the infected host. Proc. Natl. Acad. Sci. USA 92:4269–4273.
41. Theisen, M., B. Frederiksen, A.-M. Lebech, J. Vuust, and K. Hansen. 1993. Polymorphism in *ospC* gene of *Borrelia burgdorferi* and immunoreactivity of OspC protein: implications for taxonomy and for use of OspC protein as a diagnostic antigen. J. Clin. Microbiol. 31:2570–2576.
42. Wallich, R., C. Brenner, M. D. Kramer, and M. M. Simon. 1995. Molecular cloning and immunological characterization of a novel linear-plasmid-encoded gene, *pG*, of *Borrelia burgdorferi* expressed only in vivo. Infect. Immun. 63:3327–3335.
43. Wallich, R., C. Helmes, U. E. Schaible, Y. Lobet, S. E. Moter, M. D. Kramer, and M. M. Simon. 1992. Evaluation of genetic divergence among *Borrelia burgdorferi* isolates by use of OspA, *fla*, HSP60, and HSP70 gene probes. Infect. Immun. 60:4856–4866.
44. Wilske, B., A. G. Barbour, S. Bergstrom, N. Burman, B. I. Restrepo, P. A. Rosa, T. Schwan, E. Soutschek, and R. Wallich. 1992. Antigenic variation and strain heterogeneity in *Borrelia* spp. Res. Microbiol. 143:583–596.